Journal of Power Sources 273 (2015) 158–161

Contents lists available at ScienceDirect

Journal of Power Sources

journal homepage: www.elsevier.com/locate/jpowsour

Short communication

Tin Dioxide as an Effective Antioxidant for Proton Exchange Membrane Fuel Cells

Shuang Ma Andersen [a, *], Casper Frydendal Nørgaard [a], Mikkel Juul Larsen [b], Eivind Skou [a]

[a] Dep. of Chemical Eng., Biotech. & Environmental Tech., University of Southern Denmark, Niels Bohrs Allé 1, DK-5230 Odense M, Denmark
[b] IRD Fuel Cells A/S, Kullinggade 31, DK-5700 Svendborg, Denmark

HIGHLIGHTS

- SnO_2 showed effective antioxidant ability in PEMFC electrodes.
- Different degradation segments were detected under different RH OCV treatments.
- Low humidity induces greater damage to the polymer under OCV.

ARTICLE INFO

Article history:
Received 12 June 2014
Received in revised form
14 August 2014
Accepted 4 September 2014
Available online 16 September 2014

Keywords:
SnO_2
Antioxidant
Radical
PEMFC
Humidity

ABSTRACT

Tin dioxide (SnO_2) containing electrodes showed significantly lower radical induced polymer degradation under single cell open circuit voltage (OCV) treatment than SnO_2 free electrodes. A backbone related segment was detected under 100% RH, and an oxygen containing side chain segment was detected under 6% RH by ^{19}F NMR. Fluoride ion release was observed in both cases. Low humidity induces greater damage to the polymer under OCV.

1. Introduction

Durability is one of the most important issues impeding fuel cell technology commercialization. Radical induced perfluorinated sulfonic acid (PFSA) polymer degradation is generally considered the most important degradation mode for the polymer electrolyte in proton exchange membrane fuel cells (PEMFCs) [1,2]. Essential radicals involved in the process are the hydroxy radical (•OH), the hydrogen radical (H•) and the peroxy radical (HOO•) [3]. Formation of the hydroxy radical, as the initiator of a series of oxidative reactions, is formed through either decomposition of hydrogen peroxide (H_2O_2) generated via two electron oxygen reduction reaction:

$$O_2 + 2H^+ + 2e^- \rightarrow H_2O_2$$

$$H_2O_2 \rightarrow 2{}^\bullet OH$$

$$H_2O_2 + {}^\bullet OH \rightarrow HOO^\bullet + H_2O$$

or direct formation from H_2 and O_2 gasses over platinum catalyst:

$$H_2 + O_2 \rightarrow 2HO^\bullet \text{ (on catalyst surface)}$$

$$2HO^\bullet + H_2 \rightarrow H_2O_2 + 2H^\bullet$$

$$H^\bullet + O_2 \rightarrow HOO^\bullet$$

Radical induced polymer degradation mechanisms commonly considered in the literature are the back bone unzipping mechanism [4] and side chain degradations at corresponding reaction sites [5,6]. Elimination of the primary radical source is the fundamental mitigation strategy. Many species have been explored for their potential as radical scavengers, e.g. CeO_2 [7–9], MnO_2 [10], metal nanoparticles (Pt, Pd, Ag, and Au) [11] etc. However, SnO_2 has

* Corresponding author. Tel.: +45 6550 9186.
E-mail address: mashu@kbm.sdu.dk (S.M. Andersen).

http://dx.doi.org/10.1016/j.jpowsour.2014.09.051
0378-7753/

not been studied for any antioxidant (or radical scavenging) activity so far. Moreover, it is low-cost and bio-compatible.

In the literature, doped or un-doped SnO_2 has been applied as catalyst support in PEMFCs [12,13] and water electrolyzers [14] with promising results. The promotion of the catalyst activity and corrosion resistance was attributed to the unique catalyst–support interactions. Besides, SnO_2 supported Pt was also reported of better CO tolerance than conventional catalysts [15]. Furthermore, SnO_2 or its hydrated form had also been used as filler in protonic conductive membranes to improve mechanical properties [16,17] and to prevent methanol crossover [17].

The dual valency of Sn can facilitate a reversible transformation of the surface composition from stoichiometric surfaces with Sn^{4+} surface cations into a reduced surface with Sn^{2+} surface cations depending on the oxygen chemical potential of the system [18]. In analogy to CeO_2 [19], the corresponding antioxidant mechanism for SnO_2 can be schematically presented as:

$$Sn^{2+} + 2^{\bullet}OH + 2H^{+} \rightarrow Sn^{4+} + 2H_2O$$

$$Sn^{4+} + 2H_2O_2 \rightarrow Sn^{2+} + 2HOO^{\bullet} + 2H^{+}$$

$$Sn^{4+} + 2HOO^{\bullet} \rightarrow Sn^{2+} + 2O_2 + 2H^{+}$$

$$Sn^{4+} + H_2 \rightarrow Sn^{2+} + 2H^{+}$$

$$2Sn^{4+} + 2H_2O \rightarrow 2Sn^{2+} + 4H^{+} + O_2$$

In this work, SnO_2 nanoparticles were introduced in the electrode structure and tested for their antioxidant ability.

2. Experimental

Platinum and Platinum–ruthenium supported on carbon black (Hispec 9000 and 10000) were purchased from Johnson Matthey. The electrodes were fabricated following a PEMFC electrode preparation recipe, where a suspension of catalyst and Nafion® ionomer in water/alcohol was coated onto a gas diffusion layer (GDL) Sigracet® 35DC (SGL Group). SnO_2 nanoparticles were generated in-situ in the electrode polymer phase through an ion exchange procedure, described in our earlier work [16]. The exchanged electrodes were rinsed with methanol and water repeatedly in order to eliminate any residual non-ion-exchanged SnO_2. The loading of SnO_2 was determined by the weight gain of the electrode, which corresponded to around 5–8% of the ionomer.

The final electrodes with or without SnO_2 were laminated on to a Nafion 212 membrane at 140 °C, 7 bar for 3 min, to produce membrane electrode assemblies (MEAs). In this manner, four types of MEAs were fabricated: 1) SnO_2 containing anode and original cathode labelled as **TAOC**; 2) original anode and SnO_2 containing cathode labelled as **OATC**; 3) SnO_2 containing anode and SnO_2 containing cathode labelled as **TATC** and 4) original anode and original cathode labelled as **OAOC,** which is also the control in the study. Fuel cell testing was performed with a single cell of dimension 2.5 × 2.5 cm^2. The cell was kept at open circuit voltage (OCV) at 100 and 6% relative humidity (RH) and 70 °C. The flows of H_2 and air applied during the OCV testing were 10 NmL min^{-1} and 20 NmL min^{-1} respectively. I–V performance was carried out at stoichiometry values of lambda H_2 = 2 and lambda air = 4. The system was controlled and monitored by an electrochemical workstation (IM6e, ZAHNER and a homebuilt setup based on MACCOR hardware).

All NMR experiments were performed in a Bruker 400 MHz NMR spectrometer with an auto-sampler. The temperature was stabilized at 25 °C. Critical parameters include D1 = 8.0 s, AQ = 0.73 s and number of scans = 32. A capillary tube containing 1% trichlorofluoromethane (CCl_3F, 0 ppm) in chloroform was used as internal reference. All reported values are normalized towards the reference. Data analysis was assisted with the software MestRe Nova®. Detection of fluoride was performed with ion chromatography (IC) using a Dionex ICS-300C ion chromatograph equipped with an IonPac® AS18 analytical column and an ED40 conductivity detector. The scanning electron microscope (SEM) was a Hitachi S-4800 system with a cold field-emission electron source for ultra-high resolution and an energy dispersive X-ray spectrometer (EDXS).

3. Results and discussion

As illustrated by SEM-EDXS in Fig. 1, tin was successfully introduced in the catalyst layer. The existence of SnO_2 and the corresponding oxidation state was also confirmed by X-ray

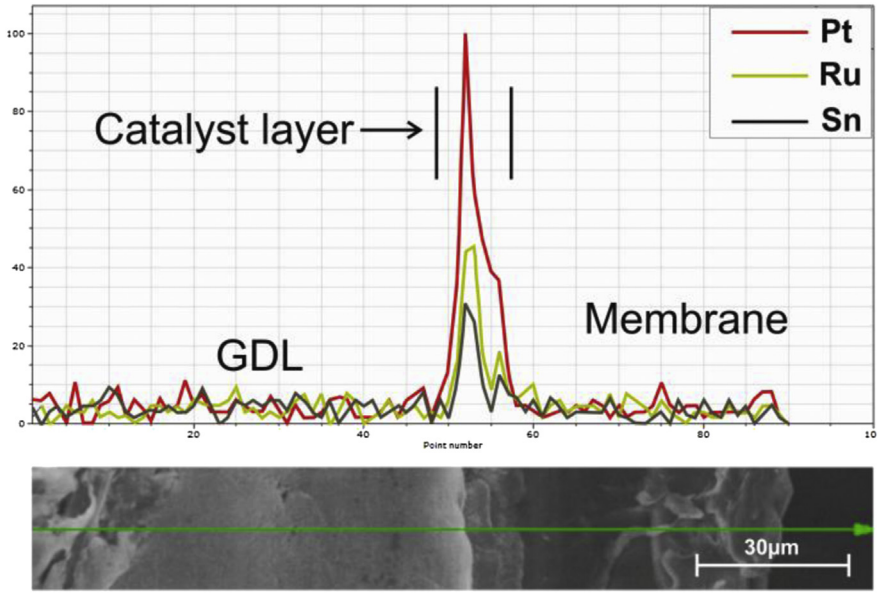

Fig. 1. SEM-EDXS cross section image and atomic line profile of MEA electrode ion exchanged with SnO_2.

photoelectron spectroscopy (data not shown). The post mortem studies of the electrodes will be the subject of a forthcoming article.

OCV performance of the 4 MEAs at 100% RH 70 °C is illustrated in Fig. 2. Apparently, all the SnO_2 containing MEAs show less degradation than the control MEA. In terms of the degradation rate (Fig. 2), the tin containing electrodes show an improvement of more than 40%. Among the three relatively stable MEAs, TAOC (SnO_2 only ion exchanged at anode) shows the highest open circuit voltage and lowest rate of degradation. This might indicate that oxidant and/or radicals are primarily generated at the anode, as also observed in our earlier study [20]. Once they are captured by the antioxidant at the anode (in comparison to at the cathode), it is more effective to extend the longevity of the cell. Large noise is observed for the OATC data and to a somewhat lesser extent for TATC. Such noise is often related to poor water management. The hydrophilic nature of SnO_2 might accelerate flooding issues at the cathode. To summarize, an MEA with SnO_2 ion exchanged only at the anode might be a good conceptual design for PEMFC of better durability and stable performance.

Current density at 0.6 V before and after OCV treatment is shown in Fig. 3. I–V curves are available in Supplementary materials. All SnO_2 containing MEAs exhibited inferior I–V performance compared to the control. This might be due to a reduction of protonic conductivity or an increase of mass transport limit, which gave rise to a higher resistance of the electrode processes. There is certainly room for electrode structure optimization, such as a fine tuning of SnO_2 loading, surface hydrophobicity improvement or minimization of Pt catalyst loss during the SnO_2 incorporation procedure. At the same time, the cell performance improves after the OCV treatment for TAOC, TATC and OAOC, in which TAOC shows the largest leap of 48% increment. The enhanced performance is often interpreted as activation or break-in: a self-organization of the three-phase boundary within the electrode structure during cell operation. This is generally related to enhancement of hydration, desorption of impurities from fabrication, activation of catalyst and pore-opening [21–23]. The exact mechanism and reaction of break–in are still not well understood; however, wetting of the electrolyte is commonly believed to be one of the most important factors for the cell activation [22]. In this sense, SnO_2 containing anode may contribute cell activation, due to water retention property of SnO_2, as reflected by TAOC. On the other hand, introducing the hydrophilic SnO_2 in the cathode may result in over-humidification of this electrode. This would lead to lower I–V performance of an activated MEA with SnO_2 containing

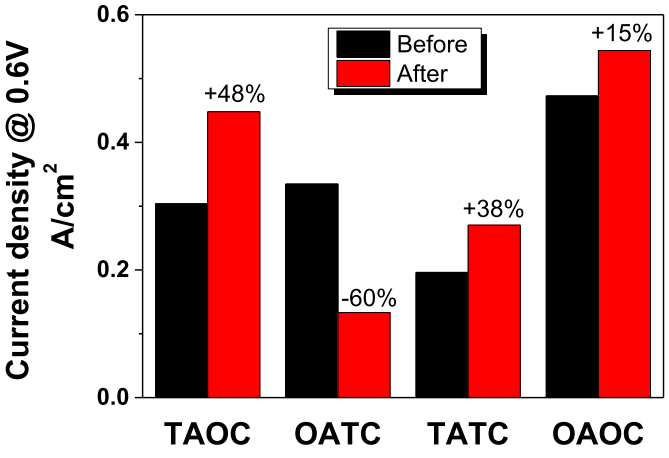

Fig. 3. Current density at 0.6 V at 100% RH before and after OCV holding treatment.

cathode, as the case for OATC (though the peculiar course of the problem can be due to many other reasons as well). Moreover, during break-in, chemical decomposition of the electrode component was also detected (see later NMR and IC measurement). The final cell performance is a combination of two opposite processes: structure self-optimization and component degradation. The greater performance improvement of TAOC than OAOC might also indicate that the SnO_2 containing anode is of better resistance toward oxidants. SnO_2 at the cathode (e.g. TATC)) apparently provides less protection against oxidants than SnO_2 at the anode; moreover, SnO_2 at the cathode (e.g. OATC) may interfere with the electrode processes. These correspond fairly well with the OCV holding measurements (Fig. 2).

Similar OCV treatment was also carried out on the 4 MEAs under 6% RH. The cell effluent water samples under both humidities were analyzed with ^{19}F NMR and IC. NMR spectra of anode water from OAOC are shown in Fig. 4. The rest of the NMR spectra are available in the Supplementary Materials.

As shown in the Fig. 4, a single sharp peak of unique position is detected for each water sample depending on the operation condition. Peak identification is carried out based on standard Nafion ionomer solution [24] (Sigma Aldrich) and commercial fluorocarbon chemicals. At 100% RH, a signal at chemical shift of −119.39 ppm is observed. The position corresponds to $-CF_2$ related bonding, which indicates that the effluent water contains

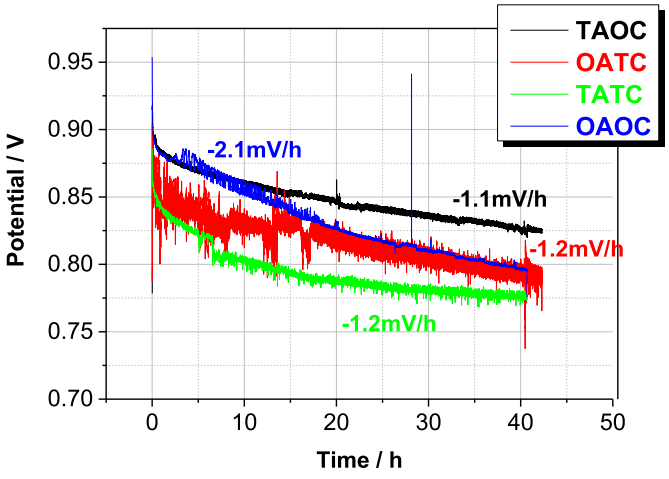

Fig. 2. OCV performance of the 4 MEAs at 100% RH.

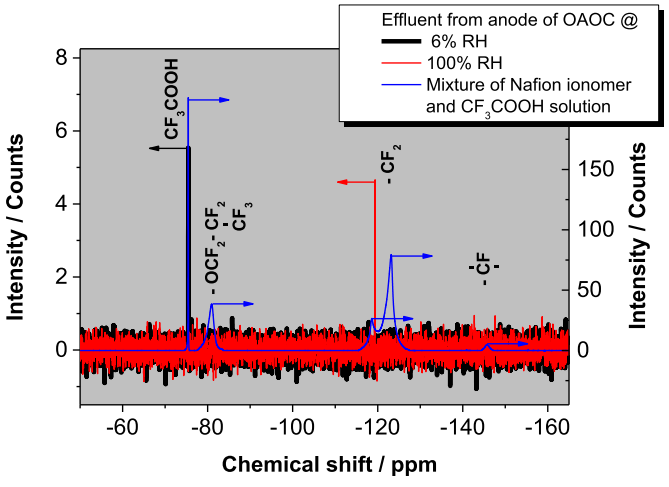

Fig. 4. ^{19}F NMR of the anode effluent water from OAOC after OCV treatment.

Table 1
Degradation product as detected by ^{19}F NMR and IC in the effluent water.

	100% RH		6% RH	
	S@-119.39[c]	F^-	S@-75.44	F^-
	%	mg L^{-1}	%	mg L^{-1}
TAOC-A[a]	B.D.L.[b]	0.23	B.D.L.	0.73
TAOC-C	B.D.L.	0.58	B.D.L.	1.98
OATC-A	B.D.L.	0.22	37.14	0.01
OATC-C	4.72	1.00	16.93	4.37
TATC-A	B.D.L.	0.22	B.D.L.	2.95
TATC-C	B.D.L.	0.26	B.D.L.	1.74
OAOC-A	26.72	3.97	38.16	4.56
OAOC-C	22.19	3.67	B.D.L.	1.40

[a] Anode of TAOC.
[b] Below Detection Limit.
[c] ^{19}F NMR signal at −119.39 ppm relative to reference compound ($CFCl_3$) at 0 ppm.

segments of fluorocarbon backbone. IC shows corresponding fluoride concentration in the effluent water. These indicate that release of fluoride ions happens at the same time as unzipping of the polymer main chain. At 6% RH, the only signal detected in ^{19}F NMR is at chemical shift −75.44 ppm, which matches well with the chemical structure of trifluoroacetic acid (CF_3COOH). This degradation product is related to Nafion side chain structure [25]. There is no clear relation between NMR and IC values for the 6% RH runs; however, this may be due to the limited amount of effluent water collectible under such dry conditions and the greater relative impact that any contaminants may have for such small samples. The corresponding decomposed segments and fluoride concentrations are summarized in Table 1.

The values clearly demonstrate that the SnO_2 containing MEAs have a substantially lower degree of polymer degradation compared to the control MEA. Best of the three, TAOC shows around 13 times lower degradation at 100% RH and around 6 times lower degradation at 6% RH than OAOC based on IC measurements. Based on NMR measurements, in all RHs, TAOC shows no sign of decomposition, in contrast to the significant amounts of degradation products observed for the control sample, OAOC. In general, the MEAs for which SnO_2 is incorporated in the anode (TAOC & TATC) show lower degradation: no polymer segments and low amounts of fluoride ion were detected in the effluent water. For the MEA with SnO_2 in the cathode (OATC), minor amounts of degradation products were observed at the cathode under 100% RH; greater degradation was observed at both electrodes under 6% RH. This might again indicate that radicals originate at the anode. Besides, there are, in most cases, higher amounts of decomposed segments detected at the anode than the cathode. Therefore, when SnO_2 is introduced at the anode, it is more efficient in capturing the radicals and preventing the degradation of the polymer.

4. Conclusion

The inexpensive and environmentally friendly SnO_2 demonstrates effective antioxidant/radical scavenging activity when it is introduced into an electrode structure using a facile ion exchange method. The tin containing electrodes showed improved stability at OCV in single cell measurement (though electrode structure optimization is still necessary). During OCV treatment, no sign or significantly lower amount of polymer degradation product was observed based on effluent water analysis by ^{19}F NMR and IC. An MEA with SnO_2 introduced in the anode is recommended for assisting activation, better durability and stable performance. The degradation product is directly related to the cell operation condition. Solely $-CF_2$ backbone block or solely trifluoroacetic acid was identified in the effluent water after OCV treatment at 100 or 6% RH, respectively. Fluoride was detected in both cases. OCV operation at low RH inflicts greater damage to the polymer. Based on the collective evidence, oxidants or radicals were primarily generated at the anode in this study.

Acknowledgements

This work was financially supported by DuraPEM II & III 2010-1-10505 & 2013-1-12064, and 4M center. Peter Lund is thanked for inspiration.

Appendix A. Supplementary data

Supplementary data related to this article can be found at http://dx.doi.org/10.1016/j.jpowsour.2014.09.051.

References

[1] L. Ghassemzadeh, K.D. Kreuer, J. Maier, K. Müller, J. Phys. Chem. C 114 (2010) 14635–14645.
[2] V.O. Mittal, H.R. Kunz, J.M. Fenton, J. Electrochem. Soc. 154 (2007) B652–B656.
[3] L. Gubler, S.M. Dockheer, W.H. Koppenol, J. Electrochem. Soc. 158 (2011) B755–B769.
[4] D.E. Curtin, R.D. Lousenberg, T.J. Henry, P.C. Tangeman, M.E. Tisack, J. Power Sources 131 (2004) 41–44.
[5] R. Uegaki, Y. Akiyama, S. Tojo, Y. Honda, S. Nishijima, J. Power Sources 196 (2011) 9856–9861.
[6] L. Ghassemzadeh, T.J. Peckham, T. Weissbach, X.Y. Luo, S. Holdcroft, J. Am. Chem. Soc. 135 (2013) 15923–15932.
[7] Z. Wang, H.L. Tang, H.J. Zhang, M. Lei, R. Chen, P. Xiao, M. Pan, J. Mem. Sci. 421–422 (2012) 201–210.
[8] S. Ghosh, S. Maity, T. Jana, J. Mater. Chem. 21 (2011) 14897–14906.
[9] P. Trogadas, J. Parrondo, V. Ramani, Electrochem. Solid-State Lett. 11 (7) (2008) B113–B116.
[10] D. Zhao, B.L. Yi, H.M. Zhang, H.M. Yu, J. Membr. Sci. 346 (2010) 143–151.
[11] P. Trogadas, J. Parrondo, F. Mijangos, V. Ramani, J. Mater. Chem. 21 (2011) 19381–19388.
[12] J. Suffner, S. Kaserer, H. Hahn, C. Roth, F. Ettingshausen, Adv. Energy Mater. 1 (2011) 648–654.
[13] K.S. Lee, I.S. Park, Y.H. Cho, D.S. Jung, N. Jung, H.Y. Park, Y.E. Sung, J. Catal. 258 (2008) 143–152.
[14] K. Kadakia, M.K. Datta, O.I. Velikokhatnyi, P. Jampani, S.K. Park, S.J. Chung, P.N. Kumta, J. Power Sources 254 (2004) 362–370.
[15] T. Takeguchi, Y. Anzai, R. Kikuchi, K. Eguchi, W. Ueda, J. Electrochem. Soc. 154 (2007) B1132–B1137.
[16] C.F. Norgaard, U.G. Nielsen, E. Skou, Solid State Ionics 213 (2012) 76–82.
[17] B. Mecheri, A. D'Epifanio, E. Traversa, S. Licoccia, J. Power Sources 178 (2008) 554–560.
[18] M. Batzill, U. Diebold, Prog. Surf. Sci. 79 (2005) 47–154.
[19] P. Trogadas, J. Parrondo, V. Ramani, ACS Appl. Mater. Interfaces 4 (2012) 5098–5102.
[20] M.J. Larsen, E.M. Skou, J. Power Sources 202 (2012) 35–46.
[21] D.E. Ramaker, A. Korovina, V. Croze, J. Melke, C. Roth, Phys. Chem. Chem. Phys. 16 (2014) 13645–13653.
[22] J.M. Jang, G.G. Park, Y.J. Sohn, S.D. Yim, C.S. Kim, T.H. Yang, J. Electrochem. Sci. Technol. 2 (2011) 131–135.
[23] M. Zhiani, S. Majidi, M.M. Taghiabadi, Fuel Cells 13 (2013) 946–955.
[24] S.M. Andersen, M. Borghei, R. Dhiman, H. Jiang, V. Ruiz, E. Kauppinen, E. Skou, Carbon 71 (2014) 218–228.
[25] C. Chen, T.F. Fuller, Polym. Degrad. Stab. 94 (2009) 1436–1447.